

MedChemComm

Accepted Manuscript



This article can be cited before page numbers have been issued, to do this please use: Y. Zhao, S. Liu, R. He, L. Kong, J. Xi, J. Sun, Y. Shao, X. Pan, J. Zhang and R. Zhuang, *Med. Chem. Commun.*, 2017, DOI: 10.1039/C7MD00409E.



This is an Accepted Manuscript, which has been through the Royal Society of Chemistry peer review process and has been accepted for publication.

Accepted Manuscripts are published online shortly after acceptance, before technical editing, formatting and proof reading. Using this free service, authors can make their results available to the community, in citable form, before we publish the edited article. We will replace this Accepted Manuscript with the edited and formatted Advance Article as soon as it is available.

You can find more information about Accepted Manuscripts in the [author guidelines](#).

Please note that technical editing may introduce minor changes to the text and/or graphics, which may alter content. The journal's standard [Terms & Conditions](#) and the ethical guidelines, outlined in our [author and reviewer resource centre](#), still apply. In no event shall the Royal Society of Chemistry be held responsible for any errors or omissions in this Accepted Manuscript or any consequences arising from the use of any information it contains.

Identification of novel *N*-acetylcysteine derivatives for the treatment of hepatocellular injury

Shourong Liu^{a, §}, Yanmei Zhao^{a, §}, Ruoyu He^a, Limin Kong^b, Jianjun Xi^a, Jingjing Sun^a, Yidan Shao^a,
Xuwang Pan^a, Jiankang Zhang^{a, *}, Rangxiao Zhuang^{a, *}

^a*Department of pharmaceutical Preparation, Hangzhou Xixi Hospital, Hangzhou 310023, Zhejiang Province, China. E-mail: zhuangrangxiao@sina.com, zjk0125@yeah.net; Tel./Fax: +86-571-8648-1960 (Rangxiao Zhuang), +86-571-8546-3955 (Jiankang Zhang)*

^b*Department of Pharmacy, The First Affiliated Hospital, College of Medicine, Zhejiang University, Hangzhou 310003, Zhejiang Province, China*

§ These authors contributed equally to this work.

Abstract: New anti-hepatocellular injury drugs with better curative effects and fewer side effects are urgently needed at present. In this study, a series of novel *N*-acetylcysteine (NAC) derivatives were designed, synthesized and biologically evaluated for their anti-hepatocellular injury activities against two different cell models. In the biological evaluation against hydrogen peroxide (H₂O₂) induced LO2 hepatocytes, half of the target compounds exhibited moderate to potent activities in improving the model cell viability, and two compounds (**6a** and **6b**) displayed more potent activities in decreasing malondialdehyde (MDA) level than that of the positive control NAC. In further 4-acetamidophenol (APAP) induced LO2 cell experiment, compounds **6a** and **6b** could not only improve the cell viability but also significantly reduce the secretion of MDA. Additionally, compound **6a** displayed excellent Caco-2 permeability and oral bioavailability in rats. All these experimental results suggested that compounds **6a** and **6b** could be served as potential lead molecules for further development of anti-hepatocellular injury drugs.

1. Introduction

Liver diseases are highly prevalent all over the world. Regardless of different etiologies, inflammation and oxidative stress (OS) are the most important pathogenetic events in hepatic diseases¹⁻³. Chemical drugs, re-oxidation after hypoxia and all kinds of acute or chronic inflammation can cause oxidative damage in hepatocytes, accompanied by the changes of cellular structure and function, which allows the liver cells to produce excessive reactive oxygen species (ROS)⁴⁻⁶. Several studies on hepatic diseases indicated that cells have intrinsic antioxidant mechanisms, such as peroxidases, catalases and superoxide dismutases to scavenge ROS. Among these antioxidant systems, the most abundant and outstanding cellular thiol antioxidant glutathione (GSH) exhibits numerous and versatile functions and therefore protects cells against oxidative stress⁷.

As an antioxidant, *N*-acetylcysteine (NAC) could directly increase the intracellular GSH, especially on hepatic tissue, and it has been in clinical practice for several decades with relatively low toxicity and good efficacy. As a small molecule, NAC has been elucidated to interact with numerous metabolic pathways including, but not limited to, regulation of cell cycle and apoptosis, carcinogenesis and tumor progression, mutagenesis, gene expression and signal transduction, immune-modulation, cytoskeleton and trafficking and mitochondrial functions⁸⁻¹⁰. The molecular mechanisms by which NAC exerts its diverse effects are complex and the insignificant routes under physiological conditions of NAC is serving as a precursor of cysteine for GSH synthesis which helping in the detoxification of reactive metabolites and scavenging of free radicals¹¹. The second important mechanism of NAC attributes to the anti-oxidative activity of its sulfhydryl group, which has a fast binding rate with $\cdot\text{OH}$, $\cdot\text{NO}_2$, $\text{CO}_3^{\cdot-}$ and thiyl radicals as well as restitutes of impaired targets in vital cellular components¹². At the meantime, the uniqueness of NAC is most probably due to efficient reduction of disulfide bonds in proteins thus altering their structures and disrupting their ligand bonding, competition with larger reducible molecules in sterical less accessible spaces. Possible chemical and biochemical routes involving NAC are summarized in **Fig. 1**¹³.

< Insert Fig. 1>

At present, administration of NAC has been mostly used as a mucolytic agent. While IV NAC is used for various types of liver injury and early stage of liver failure on the basis of comprehensive treatment in order to reduce bilirubin and increase prothrombin activity¹⁴. According to the literature, the human plasma terminal half-life of NAC after a single intravenous administration is 5.6 h where 30% of the drug is cleared by renal excretion. NAC's oral bioavailability is less than 5%, which is mainly thought to be associated with its *N*-deacetylation in the intestinal mucosa and first pass metabolism in the liver¹⁵. Researches indicated that NAC is negatively charged under the physiological condition and its neutral, membrane permeating form, constitutes as little as 0.001% of the total NAC¹⁶. Therefore, in order to achieve a certain well clinical efficacy, higher doses and longer treatment cycles should be performed, which also bring more drug toxicity risks. The side effects that accompany the use of a high dose of IV NAC includes rash, pruritus, angioedema and bronchospasm, while oral administration of NAC may be associated with vomiting and diarrhea along with an unpleasant odor.

Therefore, more effective and safer drugs are urgently required, which would be of great value for the treatment of various diseases, especially for liver injury. To improve the stability and activity of NAC, structure optimization was performed at the carboxyl, sulfhydryl and acetyl groups in this research (**Fig. 2**). Firstly, different carboxylic esters of NAC were designed and synthesized to increase the molecular permeation rate through the biological membranes by adjusting the molecule PKa. Additionally, methyl-substituted thiol could not only prevent the self-oxidation and improve the stability of the compound, but also play antioxidant effect after de-methylation by demethylase in vivo¹⁷. Finally, in order to prevent NAC from *N*-deacetylation in the intestinal mucosa and first pass metabolism in the liver, acetyl was replaced with other more stable acyl, which was expected to prolong the compound retention time in vivo and improve its bioavailability, thus overcome the adverse side effects of this drug.

< Insert Fig. 2>

2. Synthesis

The synthetic route for all the target compounds was outlined in **Scheme 1**. Firstly, Fmoc-Cys(Me)-OH

treated with corresponding carboxylic acid or ester at the presence of N, N-diisopropylethylamine (DIEA) and *N*-methylmorpholine (NMM) to give the target compounds **2a-e** by using standard Fmoc-chemistry. The target compounds **2a-e** were also important intermediates for the next step, which were then treated with HCl and MeOH to afford the methyl ester analogues **3a-e**. As illustrated in **Scheme 1**, treatment of **2a-e** with 2-tert-butyl-1, 3-diisopropyl-isourea provided the tert-butyl ester compounds **4a-e**, while reacted with methylamine hydrochloride, cyclohexylamine and aniline afforded target compounds **5a-c** and **6a-c** respectively, with proper reagents and conditions. Treatment of **2a-e** with aniline and HATU afforded the target compounds **7a** and **7b** with the structure of phenyl amide. Commercially available N-(tert-butoxycarbonyl)-S-methyl-L-cysteine **8** was converted to phenyl amide **9** in the presence of NMM and IBCF at 15 °C which was then deprotected with TFA to afford the amine **10**. Subsequently, condensation reaction of compounds **10** and benzoyl chloride provided the target compound **7c**.

< Insert Scheme 1 >

3. Pharmacology

3. 1 Cell viabilities and MDA measurement on H₂O₂ induced LO2 cell injury model

Human hepatocytes cell line, LO2, was used to build hepatocytes injury model by H₂O₂ treatment. Cell Counting Kit-8 (CCK-8) was utilized to detect cell proliferation and determine the optimal damage condition. All the target compounds were screened for their cell viabilities on this model using NAC as positive control, and the results are illustrated in **Fig. 3**.

As the results displayed in **Fig. 3**, compared with the model group, part of the target compounds (**2a**, **2b**, **2c**, **2d**, **5c**, **6a**, **6b** and **7a**) exhibited moderate to potent cell protective and repair effects against H₂O₂ treated LO2 cells. In **Fig. 3 (a)**, compounds **2a-e** had a slight improvement on cell viability when the carboxyl groups were retained and different substituents were introduced in R₁ position, while compounds **3a-e** with carboxylic methyl ester had slight inhibitory effects on cell proliferation. Additionally, compound **2a** could slightly improve the cell viability and reduce the MDA level, which indicated that the increase of the antioxidant damage ability at the cell level was limited after the introduction of methyl at R₂ position compared with NAC. In **Fig. 3 (b)**, the inhibition of cell viability increased from compound **4a** to **4e** with tert-butyl ester substituted at R₃ position. On the contrary, the

inhibitory activity decreased from compound **5a** to **5c** with formamide at R₃ position, which indicated that the structure-activity relationship of these two series of compounds is not clear and compounds **4a-e** have a certain degree of cytotoxicities. Among the formamide derivatives (**5a-c**), compound **5c** with phenyl at R₁ position has a certain recovery effect on cell viability, which displayed more potent cell protective activity than compounds **5a** and **5b**. Compounds **6a-c** and **7a-c** with different substituents at R₁ position, displayed the same regularity, in which methyl replaced analogues (**6a** and **7a**) exhibited more potent cell protective activities than ethyl substituted compounds (**6b** and **7b**), and compounds with benzene at this position (**6c** and **7c**) displayed the worst potent activities. These data also suggested that minor changes at R₁ position could greatly influence the cell viabilities of the target compounds (**4a-b**, **4d**, **6a-c** and **7a-c**) when R₃ was substituted with tert-butyl, phenyl or cyclohexyl. Among all these derivatives (except **2a** and **5a**), the ones with methyl substituted at R₁ position displayed more potent activities than other ones. The most potent compound **6a**, whose cell protective and repair activity was superior to model group, deserved further study with regard to its application potential in the treatment of anti-hepatic injury.

< Insert Fig. 3 (a) >

< Insert Fig. 3 (b) >

< Insert Fig. 3 (c) >

Based on the results of cell viabilities of all the target compounds, selected analogues (**2a-e**, **5b-c**, **6a-b** and **7a**) were screened for their effects on malondialdehyde (MDA) secretion in H₂O₂ treated LO2 cells by Lipid oxidation (MDA) Assay Kit using NAC as positive control. The results were shown in **Fig. 4**. Except for compound **5c**, all the selected compounds could decrease the MDA level in the LO2 cells injured by H₂O₂ compared to that of the model group. In particular, compounds **6a**, **6b** and **7a** exhibited more potent MDA secretion inhibitory activities than that of the positive control, which indicated that these active compounds could protect injured liver cells through inhibition of MDA secretion.

< Insert Fig. 4 >

3.2 Cell viabilities and MDA measurement on APAP induced LO2 cell injury model

To further confirm the cell protective activities of compounds **6a**, **6b** and **7a** on oxidative injured liver cells, an additional experiment was performed to determine the effects of the three selected compounds on APAP induced LO2 injured cells. As displayed in **Fig. 5**, compared with the model group, compounds **6a** and **6b** exhibited moderate improvement on cell viability while **7a** have almost no effect. At the same time, effects of compounds **6a**, **6b** and **7a** on MDA secretion in APAP treated LO2 cells were studied by using Lipid oxidation (MDA) Assay Kit. As shown in **Fig. 6**, compared with the model group, compounds **6a**, **6b** and **7a** could significantly reduce the level of MDA in the APAP treated LO2 cells. However, the recovery abilities of compounds **6a** and **6b** was no better than that of the positive control NAC.

< Insert Fig. 5>

< Insert Fig. 6>

4. ADME properties

The preliminary ADME profiles of compound **6a** were evaluated by determining its Caco-2 permeability (**Table 1**) and pharmacokinetic properties (**Table 2**). As displayed in **Table 1**, compound **6a** exhibited a better Caco-2 permeability compared to that of the positive control NAC, which also validated the initial structural optimization ideas. In addition, as the pharmacokinetic data depicted in **Table 2**, the terminal half-life of compound **6a** after a single oral administration was 5.62 h and its oral bioavailability could reach 52.8% in SD rats.

< Insert Table 1>

< Insert Table 2>

4. Conclusion

A novel series of NAC derivatives were designed, synthesized and biologically evaluated for their cell protective activities on H₂O₂ treated LO2 hepatocytes, and half of the derivatives exhibited moderate to potent activities. Additionally, selected ten compounds were further screened for their effect on MDA secretion. What encouraged us was that three compounds (**6a**, **6b** and **7a**) exhibiting more potent activities than that of the positive control NAC were successively obtained. In further APAP treated LO2 cells study, compounds **6a** and **6b** could not only improve the cell viability but also significantly reduce the level of MDA. However, the effect of different substituents on the selectivity and pharmacological activity of target compounds was not very clear in this study, and the main reason for the unclear structure-activity relationship was that the target compounds were pharmacological screened on the cell model. The cell viabilities of various target compounds were affected by both the electronegativity and size of different substituents and the physicochemical properties of these compounds. If the test was carried out at a molecular level, the structure-activity relationship would be more explicit, and we will focus on this issue in subsequent research.

In the ADME studies, compound **6a** showed excellent Caco-2 permeability and good oral bioavailability in rats. Overall, although we did not get compound significantly superior to the precursor NAC in pharmacodynamics, the membrane permeability and pharmacokinetic profiles of compound **6a** was significantly better than NAC. All these results suggested that compounds **6a** could be a potential lead molecule for further structural optimization and investigation.

5. Experimental procedures

5.1 Chemistry, general methods

Mass spectra (MS) were taken in ESI mode on Agilent 1100 LC-MS (Agilent, Palo Alto, CA, U.S.A.). ¹H NMR and ¹³C NMR spectra were recorded on Bruker 400 MHz spectrometers (Bruker Bioscience, Billerica, MA, USA) with TMS as an internal standard and CDCl₃ or DMSO-*d*₆ as solvents. Coupling constants (*J*) were reported in Hertz (Hz). Splitting patterns were designated as singlet (s), broad singlet (brs), doublet (d), double doublet (dd), triplet (t), quartet (q), and multiplet (m). All materials were obtained from commercial suppliers and were used without further purification. Reaction time and purity of the products were monitored by TLC on FLUKA silica gel aluminum cards (0.2 mm thickness) with fluorescent indicator 254 nm. Column chromatography was run on silica gel (200-300 mesh) from Qingdao Ocean Chemicals (Qingdao, Shandong, China). All yields were unoptimized and generally represent the result of a single experiment.

5.2 Synthetic procedures

5.2.1 Method for the preparation of compound *N*-acetyl-*S*-methyl-L-cysteine (**2a**)

Compound **2a** was synthesized using standard Fmoc chemistry. The mixture of Chlorotriyl Chloride (CTC) Resin (18.2 mmol), Fmoc-Cys(Me)-OH (5.2 g, 41.6 mmol, 0.8 eq) and DCM (200.0 mL) were stirred at 25 °C in vessel for 12 h under N₂ atmosphere and then DIEA (3.2 eq) was added dropwise and stirred for another 2 h. Then, MeOH (20.0 mL) was added and stirred for 30 min, and the mixture was washed with DMF (10×5.0 ml). Subsequently, 20% piperidine/DMF was drained and reacted for 30 min, and the mixture was then washed with DMF again (10×5.0 ml). A solution of 85% DMF/10% Acetyl acetate/5% NMM (200 mL) was added and reacted under N₂ atmosphere for 0.5 h. Finally, 20% piperidine in DMF was used for Fmoc deprotection, and the reaction lasted for 30 min. The coupling reaction was monitored by ninhydrin test, and the resin was washed with DMF (10×5.0 ml). In peptide cleavage and purification phase, cleavage buffer (80% DCM/ 20% 1, 1, 1, 3, 3, 3-hexafluoro-2-propanol (HFIP)) was added to the flask at room temperature for 0.5 h. Then the reaction mixture was filtered and the HFIP-mixture was concentrated under reduced pressure to remove solvent. The crude peptide was purified by PreHPLC (A: 0.1% TFA in H₂O, B: acetonitrile) to give the compound **2a**.

White solid; Yield: 91%; Purity: 95%; ¹H NMR (400MHz, *d*₆-DMSO): δ = 8.23 (d, 1H, *J* = 8.1 Hz, NH), 4.40 (m, 1H, *J* = 8.3, 5.0 Hz, CH), 2.77 (ddd, 2H, *J* = 22.0, 13.6, 6.7 Hz, CH₂), 2.07 (s, 3H, CH₃), 1.86 (s, 3H, CH₃); ¹³C NMR (101MHz, DMSO): δ = 172.78, 169.77, 52.01, 35.54, 22.82, 15.68; HRMS (ES⁺) *m/z* 178.0452 (178.0460 Calcd for C₆H₁₁NO₃S M + H).

5.2.2 Preparation of compounds **2b-e**

Peptides **2b-e** were also synthesized using standard Fmoc chemistry. The mixture of CTC Resin (18.2 mmol), Fmoc-Cys(Me)-OH (5.2 g, 41.6 mmol, 0.8 eq) and DCM (200.0 mL) were stirred at 25 °C in vessel for 12 h under N₂ atmosphere and then DIEA (3.2 eq) was added dropwise and stirred for 2 h. MeOH (20.0 mL) was added and mixed for 30 min, and the mixture was washed with DMF (10×5.0 ml). After that, 20% piperidine/ DMF was drained and reacted for 30 min, and washed with DMF again (10×5.0 ml), and then corresponding acid was added and mixed for 30 s. The activation buffer was added under N₂ atmosphere for 0.5 h. Finally, 20% piperidine in DMF was used for Fmoc deprotection for 30 min. The coupling reaction was monitored by ninhydrin test, and the resin was washed with

DMF (10×5.0 ml). In peptide cleavage and purification phase, cleavage buffer (80% DCM/ 20% HFIP) was added to the flask at room temperature for 0.5 h. Then the reaction mixture was filtered and the HFIP-mixture was concentrated under reduced pressure to remove solvent. The crude peptides were purified by PreHPLC (A: 0.1% TFA in H₂O, B: acetonitrile) to give the compounds **2b-e**.

S-methyl-*N*-propionyl-L-cysteine (**2b**)

White solid; Yield: 80%; Purity: 96%; ¹H NMR (400MHz, *d*₆-DMSO): δ = 8.13 (d, 1H, *J* = 8.1 Hz, NH), 4.40 (td, 1H, *J* = 8.3, 5.0 Hz, CH), 2.77 (ddd, 2H, *J* = 22.2, 13.7, 6.8 Hz, CH₂), 2.14 (q, 2H, *J* = 7.6 Hz, CH₂), 2.07 (s, 3H, CH₃), 0.99 (t, 3H, *J* = 7.6 Hz, CH₃); ¹³C NMR (101MHz, DMSO): δ = 173.47, 172.84, 51.94, 35.56, 28.64, 15.69, 10.24; HRMS (ES⁺) *m/z* 192.0608 (192.0616 Calcd for C₇H₁₃NO₃S M + H).

N-(cyclohexanecarbonyl)-*S*-methyl-L-cysteine (**2c**)

White solid; Yield: 86%; Purity: 95%; ¹H NMR (400MHz, *d*₆-DMSO): δ = 7.15 (d, 1H, *J* = 6.4 Hz, NH), 3.87 (dd, 1H, *J* = 10.9, 5.4 Hz, CH), 2.83 (ddd, 2H, *J* = 18.5, 13.1, 5.0 Hz, CH₂), 2.11 (t, 1H, *J* = 11.1 Hz, CH), 1.97 (s, 3H, CH₃), 1.77 – 1.53 (m, 5H, Cyclohexane-H), 1.35 – 1.10 (m, 5H, Cyclohexane-H); ¹³C NMR (101MHz, DMSO): δ = 174.38, 173.14, 53.95, 44.66, 37.50, 30.06, 29.64, 26.03, 25.77, 25.71, 16.16; HRMS (ES⁺) *m/z* 246.1090 (246.1086 Calcd for C₁₁H₁₉NO₃S M + H).

N-benzoyl-*S*-methyl-L-cysteine (**2d**)

White solid; Yield: 81%; Purity: 95%; ¹H NMR (400MHz, *d*₆-DMSO): δ = 7.95 (d, 1H, *J* = 6.4 Hz, NH), 7.84 – 7.72 (m, 2H, Ar-H), 7.58 – 7.38 (m, 3H, Ar-H), 4.10 (dd, 1H, *J* = 10.3, 6.1 Hz, CH), 2.98 (ddd, 2H, *J* = 19.2, 13.2, 5.1 Hz, CH₂), 2.01 (s, 3H, CH₃); ¹³C NMR (101MHz, DMSO): δ = 173.11, 165.60, 135.50, 131.43, 128.83, 127.35, 54.57, 37.34, 15.99; HRMS (ES⁺) *m/z* 240.0604 (240.0616 Calcd for C₁₁H₁₃NO₃S M + H).

N-(4-fluorobenzoyl)-*S*-methyl-L-cysteine (**2e**)

White solid; Yield: 81%; Purity: 95%; ¹H NMR (400MHz, *d*₆-DMSO): δ = 7.98 (d, 1H, *J* = 6.6 Hz, NH), 7.88 (dd, 2H, *J* = 8.7, 5.6 Hz, Ar-H), 7.29 (t, 2H, *J* = 8.9 Hz, Ar-H), 4.12 (dd, 1H, *J* = 8.5, 4.5 Hz, CH), 2.96 (ddd, 2H, *J* = 19.8, 13.2, 5.4 Hz, CH₂), 2.01 (s, 3H, CH₃); ¹³C NMR (101MHz, DMSO): δ = 172.96, 164.61, 130.04, 129.96, 115.79, 115.57, 54.64, 37.37, 15.91; HRMS (ES⁺) *m/z* 258.0528 (258.0522 Calcd for C₁₁H₁₂NO₃S M + H).

5.2.3 General methods for preparation of the target compounds **3a-e**

An appropriate intermediates **2a-2e** (1.1 mmol) in HCl/ MeOH (4 M, 5.0 mL) was stirred at 15 °C for 3

h. The solvent was removed under reduced pressure and the residue was purified by pre-HPLC (acid condition, TFA) to give desired compounds **3a-e**.

methyl *N*-acetyl-*S*-methyl-L-cysteinate (**3a**)

White solid; Yield: 78%; Purity: 97%; ^1H NMR (400 MHz, MeOD) : δ = 4.65 (dd, 1H, J = 8.2, 5.2 Hz, CH), 3.75 (s, 3H, CH₃), 2.89 (ddd, 2H, J = 22.2, 13.9, 6.8 Hz, CH₂), 2.13 (s, 3H, CH₃), 2.01 (s, 3H, CH₃); ^{13}C NMR (101MHz, DMSO): δ = 171.87, 169.85, 52.48, 51.98, 35.24, 22.73, 15.58; HRMS (ES⁺) m/z 192.0610 (192.0616 Calcd for C₇H₁₃NO₃S M + H).

methyl *S*-methyl-*N*-propionyl-L-cysteinate (**3b**)

White solid; Yield: 84%; Purity: 99%; ^1H NMR (400 MHz, MeOD) : δ = 4.65 (dd, 1H, J = 8.4, 5.2 Hz, CH), 3.75 (s, 3H, CH₃), 2.89 (ddd, 2H, J = 22.3, 13.9, 6.8 Hz, CH₂), 2.29 (q, 2H, J = 7.6 Hz, CH₂), 2.13 (s, 3H, CH₃), 1.15 (t, J = 7.6 Hz, 3H, CH₃); ^{13}C NMR (101MHz, DMSO): δ = 173.56, 171.93, 52.46, 51.94, 35.25, 28.56, 15.59, 10.17; HRMS (ES⁺) m/z 206.0787 (206.0773 Calcd for C₈H₁₅NO₃S M + H).

methyl *N*-(cyclohexanecarbonyl)-*S*-methyl-L-cysteinate (**3c**)

White solid; Yield: 86%; Purity: 99%; ^1H NMR (400 MHz, MeOD) : δ = 4.62 (dd, 1H, J = 8.6, 5.2 Hz, CH), 3.75 (s, 3H, CH₃), 2.89 (ddd, 2H, J = 22.5, 13.9, 6.9 Hz, CH₂), 2.29 (tt, 1H, J = 11.7, 3.3 Hz, CH), 1.88 – 1.67 (m, 5H, Cyclohexane-H), 1.53 – 1.21 (m, 5H, Cyclohexane-H); ^{13}C NMR (101MHz, DMSO): δ = 175.83, 171.96, 52.44, 51.78, 44.00, 35.19, 29.62, 29.46, 25.90, 25.65, 25.16, 15.56; HRMS (ES⁺) m/z 260.1228 (260.1242 Calcd for C₁₂H₂₁NO₃S M + H).

methyl *N*-benzoyl-*S*-methyl-L-cysteinate (**3d**)

White solid; Yield: 81%; Purity: 98%; ^1H NMR (400 MHz, MeOD) : δ = 8.75 (d, 1H, J = 7.0 Hz, NH), 7.87 (dd, 2H, J = 5.3, 3.3 Hz, Ar-H), 7.62 – 7.54 (m, 1H, Ar-H), 7.54 – 7.43 (m, 2H, Ar-H), 4.87 – 4.82 (m, 1H, CH), 3.79 (s, 3H, CH₃), 3.05 (ddd, 2H, J = 23.0, 13.9, 7.1 Hz, CH₂), 2.17 (s, 3H, CH₃); ^{13}C NMR (101MHz, DMSO): δ = 171.85, 166.91, 134.04, 132.07, 128.82, 127.91, 52.59, 52.57, 34.85, 15.45; HRMS (ES⁺) m/z 254.0763 (254.0773 Calcd for C₁₂H₁₅NO₃S M + H).

methyl *N*-(4-fluorobenzoyl)-*S*-methyl-L-cysteinate (**3e**)

White solid; Yield: 79%; Purity: 98%; ^1H NMR (400 MHz, MeOD) : δ = 8.78 (d, 1H, J = 7.2 Hz, NH), 8.02 – 7.80 (m, 2H, Ar-H), 7.23 (dd, 2H, J = 9.7, 7.8 Hz, Ar-H), 4.86 – 4.80 (m, 1H, CH), 3.78 (s, 3H, CH₃), 3.04 (ddd, 2H, J = 23.1, 13.9, 7.1 Hz, CH₂), 2.17 (s, 3H, CH₃); ^{13}C NMR (101MHz, DMSO): δ = 171.62, 165.97, 130.66, 130.57, 115.91, 115.69, 52.61, 52.60, 34.82, 15.43; HRMS (ES⁺) m/z 272.0660

(272.0678 Calcd for $C_{12}H_{14}NO_3S$ M + H).

5.2.4 General procedure for the preparation of **4a-e**

A solution of appropriate intermediates **2a-e**, 2-tert-butyl-1, 3-diisopropyl-isourea (507.8 mg, 2.5 mmol) in DCM (5.0 mL) was stirred at 80°C for 12h. Then 2-tert-butyl-1, 3-diisopropyl-isourea (507.0 mg, 2.5 mmol) was added and the resulting mixture was stirred at 80 °C for another 12 h. The mixture was cooled to room temperature, filtered, and the filtrate was concentrated in vacum. The residue was purified by pre-HPLC (acid condition, TFA) to get desired compounds **4a-e**.

tert-butyl *N*-acetyl-*S*-methyl-L-cysteinate (**4a**)

Colorless oil; Yield: 65%; Purity: 99%; 1H NMR (400 MHz, MeOD) : δ = 4.51 (dd, 1H, J = 8.2, 5.3 Hz, CH), 2.85 (ddd, 2H, J = 21.9, 13.8, 6.8 Hz, CH_2), 2.14 (s, 3H, CH_3), 2.01 (s, 3H, CH_3), 1.50 (s, 9H, C_4H_9); ^{13}C NMR (101MHz, DMSO): δ = 170.49, 169.78, 81.45, 52.73, 35.49, 28.08, 22.77, 15.68; HRMS (ES^+) m/z 178.0456 (178.0460 Calcd for $C_6H_{11}NO_3S$ M + H- C_4H_9).

tert-butyl *S*-methyl-*N*-propionyl-L-cysteinate (**4b**)

Yellow oil; Yield: 72%; Purity: 98%; 1H NMR (400 MHz, MeOD) : δ = 4.57 (s, 1H, CH), 3.08 – 2.76 (m, 2H, CH_2), 2.43 – 2.28 (m, 2H, CH_2), 2.21 (d, J = 2.0 Hz, 3H, CH_3), 1.56 (s, 9H, C_4H_9), 1.30 – 1.15 (m, 3H, CH_3); ^{13}C NMR (101MHz, DMSO): δ = 173.50, 170.50, 81.38, 52.69, 35.46, 28.64, 28.08, 15.69, 10.28; HRMS (ES^+) m/z 192.0602 (192.0616 Calcd for $C_7H_{13}NO_3S$ M + H- C_4H_9).

tert-butyl *N*-(cyclohexanecarbonyl)-*S*-methyl-L-cysteinate (**4c**)

Yellow oil; Yield: 71%; Purity: 95%; 1H NMR (400 MHz, MeOD) : δ = 8.13 (d, 1H, J = 6.8 Hz, NH), 4.47 (td, 1H, J = 8.2, 5.2 Hz, CH), 2.86 (ddd, 2H, J = 22.2, 13.7, 6.8 Hz, CH_2), 2.29 (tt, 1H, J = 11.8, 3.3 Hz, CH), 2.13 (s, 1H, CH_3), 1.77 (dd, 5H, J = 40.8, 9.4 Hz, Cyclohexane-H), 1.57 – 1.16 (m, 14H, Cyclohexane-H+ C_4H_9); ^{13}C NMR (101MHz, DMSO): δ = 175.68, 170.51, 81.25, 52.59, 44.01, 35.31, 29.61, 29.52, 28.08, 25.91, 25.66, 25.63, 15.65; HRMS (ES^+) m/z 246.1094 (246.1086 Calcd for $C_{11}H_{19}NO_3S$ M + H- C_4H_9).

tert-butyl *N*-benzoyl-*S*-methyl-L-cysteinate (**4d**)

Yellow oil; Yield: 61%; Purity: 99%; 1H NMR (400 MHz, MeOD) : δ = 8.64 (d, 1H, J = 7.0 Hz, NH), 7.92 – 7.79 (m, 2H, Ar-H), 7.65 – 7.43 (m, 3H, Ar-H), 4.76 – 4.64 (m, 1H, CH), 3.02 (ddd, 2H, J = 22.8, 13.8, 7.1 Hz, CH_2), 2.17 (s, 3H, CH_3), 1.51 (s, 9H, C_4H_9); ^{13}C NMR (101MHz, DMSO): δ = 170.44, 166.95, 134.33, 131.95, 128.79, 127.86, 81.52, 53.33, 35.01, 28.11, 15.50; HRMS (ES^+) m/z 240.060 (240.0616 Calcd for $C_{11}H_{13}NO_3S$ M + H- C_4H_9).

tert-butyl *N*-(4-fluorobenzoyl)-*S*-methyl-L-cysteinate (**4e**)

Yellow oil; Yield: 75%; Purity: 99%; ^1H NMR (400 MHz, MeOD) : δ = 8.67 (d, 1H, J = 7.4 Hz, NH), 8.00 – 7.81 (m, 2H, Ar-H), 7.33 – 7.12 (m, 2H, Ar-H), 4.69 (ddd, 1H, J = 9.0, 8.0, 5.1 Hz, CH), 3.02 (tt, 2H, J = 22.9, 6.8 Hz, CH₂), 2.17 (s, 3H, CH₃), 1.51 (s, 9H, C₄H₉); ^{13}C NMR (101MHz, DMSO): δ = 170.39, 165.89, 130.60, 130.51, 115.86, 115.64, 81.57, 53.37, 35.01, 28.10, 15.49; HRMS (ES⁺) m/z 258.0536 (258.0522 Calcd for C₁₁H₁₂NO₃S M + H-C₄H₉).

5.2.5 Preparation of compounds **5a**, **5b** and **5c**

To a mixture of appropriate intermediate (**2b**, **2c** or **2e**, 1.2 mmol), EDCI (189.2 mg, 1.5 mmol), DIEA (315.4 mg, 2.4 mmol), HOBT (197.8 mg, 1.5 mmol) in DMF (5.0 mL) was added methanamine hydrochloride (90.6 mg, 1.3 mmol) at 15 °C. Then the mixture was stirred at 15 °C for 16 h, diluted with DCM (100.0 mL), washed with 1 M HCl (1×20.0 mL), H₂O (1×20.0 mL), brine (1×20.0 mL), dried over anhydrous Na₂SO₄, and concentrated under reduced pressure. The residue was purified by pre-HPLC (acid condition, TFA) to get desired compounds **5a**, **5b** and **5c** as white solids.

(*R*)-*N*-methyl-3-(methylthio)-2-propionamidopropanamide (**5a**)

White solid; Yield: 82%; Purity: 97%; ^1H NMR (400 MHz, MeOD) : δ = 8.08 (s, 1H, NH), 4.50 (ddd, 1H, J = 8.1, 7.0, 4.3 Hz, CH), 2.96 – 2.65 (m, 5H, CH₂+CH₃), 2.30 (q, J = 7.6 Hz, 2H, CH₂), 2.12 (s, 3H, CH₃), 1.15 (t, J = 7.6 Hz, 3H, CH₃); ^{13}C NMR (101MHz, DMSO): δ = 173.55, 171.22, 52.24, 36.30, 28.70, 26.07, 15.52, 10.20; HRMS (ES⁺) m/z 205.0516 (205.0932 Calcd for C₈H₁₆N₂O₂S M + H).

(*R*)-*N*-(1-(methylamino)-3-(methylthio)-1-oxopropan-2-yl)cyclohexanecarboxamide (**5b**)

White solid; Yield: 79%; Purity: 98%; ^1H NMR (400 MHz, MeOD) : δ = 7.96 (d, 1H, J = 7.8 Hz, NH), 4.55 – 4.40 (m, 1H, CH), 2.96 – 2.65 (m, 5H, CH₂+CH₃), 2.29 (tt, 1H, J = 11.7, 3.4 Hz, CH), 2.12 (s, 3H, CH₃), 1.91-1.65 (m, 5H, Cyclohexane-H), 1.53-1.18 (m, 5H, Cyclohexane-H); ^{13}C NMR (101MHz, DMSO): δ = 175.67, 171.28, 52.01, 44.15, 36.34, 29.94, 29.32, 26.08, 25.94, 25.77, 25.63, 15.48; HRMS (ES⁺) m/z 259.1419 (259.1402 Calcd for C₁₂H₂₂N₂O₂S M + H).

(*R*)-*N*-(1-(methylamino)-3-(methylthio)-1-oxopropan-2-yl)benzamide (**5c**)

White solid; Yield: 89%; Purity: 99%; ^1H NMR (400 MHz, MeOD) : δ = 7.89 (dd, 2H, J = 5.3, 3.3 Hz, Ar-H), 7.63 – 7.43 (m, 3H, Ar-H), 4.74 (dd, 1H, J = 8.6, 5.8 Hz, CH), 2.97 (ddd, 2H, J = 22.5, 13.9, 7.2 Hz, CH₂), 2.79 (s, 3H, CH₃), 2.17 (s, 3H, CH₃); ^{13}C NMR (101MHz, DMSO): δ = 171.21, 166.82, 134.47, 131.83, 128.65, 128.03, 53.07, 36.02, 26.18, 15.42; HRMS (ES⁺) m/z 253.0912 (253.0932

Calcd for $C_{12}H_{16}N_2O_2S$ M + H).

5.2.6 General procedure for the synthesis of **6a**, **6b** and **6c**

To a solution of appropriate intermediate (**2a**, **2b** or **2e**, 1.1 mmol), NMM (137.2 mg, 1.4 mmol) in THF (4.0 mL) was added isobutyl chloroformate (IBCF) (169.8 mg, 1.2 mmol) dropwise at 0 °C. After addition, the mixture was stirred at 0 °C for 1 h and cyclohexanamine (123.3 mg, 1.2 mmol) was added at the same temperature. The resulting mixture was stirred at 0 °C for another 1 h, which was then diluted with DCM (50.0 mL), washed with 1 M HCl (1×20.0 mL), brine (1×20.0 mL), dried over anhydrous Na_2SO_4 , and concentrated under reduced pressure. The residue was purified by pre-HPLC (acid condition, TFA) to obtain the desired compounds **6a**, **6b** and **6c** as white solid.

(*R*)-2-acetamido-*N*-cyclohexyl-3-(methylthio)propanamide (**6a**)

White solid; Yield: 68%; Purity: 92%; 1H NMR (400 MHz, MeOD) : δ = 8.12 (dd, 1H, J = 55.0, 7.6 Hz, NH), 4.50 (td, 1H, J = 7.9, 4.7 Hz, CH), 3.65 (tdt, 1H, J = 11.6, 7.9, 3.9 Hz, CH), 2.78 (ddd, 2H, J = 21.6, 13.7, 7.1 Hz, CH_2), 2.14 (s, 3H, CH_3), 2.01 (s, 3H, CH_3), 1.92 – 1.59 (m, 5H, Cyclohexane-H), 1.44 – 1.14 (m, 5H, Cyclohexane-H); ^{13}C NMR (101MHz, DMSO): δ = 169.86, 169.52, 52.28, 48.08, 36.62, 32.77, 32.62, 25.66, 24.99, 24.93, 22.97, 15.60; HRMS (ES^+) m/z 259.1416 (259.1402 Calcd for $C_{12}H_{22}N_2O_2S$ M + H).

(*R*)-*N*-cyclohexyl-3-(methylthio)-2-propionamidopropanamide (**6b**)

White solid; Yield: 63%; Purity: 99%; 1H NMR (400 MHz, MeOD) : δ = 4.50 (dd, 1H, J = 7.7, 6.6 Hz, CH), 3.66 (td, 1H, J = 10.7, 5.6 Hz, CH), 2.79 (ddd, 2H, J = 21.6, 13.7, 7.2 Hz, CH_2), 2.28 (q, J = 7.6 Hz, 2H, CH_2), 2.14 (s, 3H, CH_3), 1.93-1.60 (m, 5H, Cyclohexane-H), 1.45-1.19 (m, 5H, Cyclohexane-H), 1.15 (t, 3H, J = 7.6 Hz, CH_3); ^{13}C NMR (101MHz, DMSO): δ = 173.27, 169.74, 52.23, 48.06, 36.62, 32.77, 32.66, 28.71, 25.66, 24.96, 24.90, 15.62, 10.30; HRMS (ES^+) m/z 273.1546 (273.1558 Calcd for $C_{13}H_{24}N_2O_2S$ M + H).

(*R*)-*N*-(1-(cyclohexylamino)-3-(methylthio)-1-oxopropan-2-yl)benzamide (**6c**)

White solid; Yield: 73%; Purity: 99%; 1H NMR (400 MHz, MeOD) : δ = 8.42 (d, 1H, J = 7.8 Hz, NH), 8.15 (d, 1H, J = 8.2 Hz, NH), 7.93-7.76 (m, 2H, Ar-H), 7.53 (dt, 3H, J = 14.9, 7.3 Hz, Ar-H), 4.80- 4.65 (m, 1H, CH), 3.77-3.60 (m, 1H, CH), 2.94 (ddd, 2H, J = 22.1, 13.8, 7.2 Hz, CH_2), 2.18 (s, 1H, CH_3), 1.95-1.62 (m, 5H, CH_3), 1.48-1.12 (m, 5H, CH_3); ^{13}C NMR (101MHz, DMSO): δ = 169.77, 166.69, 134.54, 131.81, 128.69, 127.95, 53.08, 48.19, 36.29, 32.78, 32.69, 25.66, 24.99, 24.95, 15.51; HRMS (ES^+) m/z 321.1552 (321.1558 Calcd for $C_{17}H_{24}N_2O_2S$ M + H).

5.2.7 General procedure for the preparation of **7a-b**

(*R*)-2-acetamido-3-(methylthio)-*N*-phenylpropanamide (**7a**)

A solution of compound **2a** (200.0 mg, 1.1 mmol), aniline (160.8 mg, 1.7 mmol), HATU (515.6 mg, 1.4 mmol) in DMF (3.0 mL) was stirred at 15 °C for 16 h. Then DMF was removed under reduced pressure. The residue was diluted with DCM (100.0 mL), washed with 1 M HCl (1×30.0 mL), H₂O (1×30.0 mL), brine (1×30.0 mL), dried over anhydrous Na₂SO₄, and concentrated under reduced pressure to get compound **7a** as a white solid.

White solid; Yield: 61%; Purity: 99%; ¹H NMR (400 MHz, MeOD) : δ = 10.02 (s, 1H, NH), 7.66-7.51 (m, 2H, Ar-H), 7.33 (dd, 2H, *J* = 10.8, 5.2 Hz, Ar-H), 7.13 (t, 1H, *J* = 7.4 Hz, Ar-H), 4.76-4.59 (m, 1H, CH), 2.90 (ddd, 2H, *J* = 21.7, 13.8, 7.2 Hz, CH₂), 2.17 (s, 3H, CH₃), 2.04 (s, 3H, CH₃); ¹³C NMR (101MHz, DMSO): δ = 169.85, 169.77, 139.25, 129.18, 123.96, 119.82, 53.36, 36.14, 22.91, 15.67; HRMS (ES⁺) *m/z* 253.0922 (253.0932 Calcd for C₁₂H₁₆N₂O₂S M + H).

(*R*)-3-(methylthio)-*N*-phenyl-2-propionamidopropanamide (**7b**)

A solution of compound **2b** (300.0 mg, 1.6 mmol), aniline (160.8 mg, 1.7 mmol), EDCI (451.5 mg, 2.4 mmol) in pyridine (5.0 mL) was stirred at 15 °C for 16 h. The solvent was removed under reduced pressure. The residue was diluted with DCM (100.0 mL), washed with 1 M HCl (1×30.0 mL), H₂O (1×30.0 mL), brine (1×30.0 mL), dried over anhydrous Na₂SO₄, and concentrated under reduced pressure. The residue was purified by pre-HPLC (acid condition, TFA) to get compound **7b** as a white solid.

White solid; Yield: 55%; Purity: 97%; ¹H NMR (400 MHz, MeOD) : δ = 10.02 (s, 1H, NH), 7.64 – 7.52 (m, 2H, Ar-H), 7.33 (dd, *J* = 10.8, 5.1 Hz, 2H, Ar-H), 7.13 (t, *J* = 7.4 Hz, 1H, Ar-H), 4.77 – 4.62 (m, 1H, CH), 2.90 (ddd, *J* = 21.8, 13.8, 7.2 Hz, 2H, CH₂), 2.32 (q, *J* = 7.6 Hz, 2H, CH₂), 2.17 (s, 3H, CH₃), 1.17 (t, *J* = 7.6 Hz, 3H, CH₃); ¹³C NMR (101MHz, DMSO): δ = 173.49, 169.90, 139.27, 129.18, 123.95, 119.81, 53.31, 36.18, 28.65, 15.68, 10.26; HRMS (ES⁺) *m/z* 267.1095 (267.1089 Calcd for C₁₃H₁₈N₂O₂S M + H).

5.2.8 Preparation of the target compound **7c**

tert-butyl (*R*)-(3-(methylthio)-1-oxo-1-(phenylamino)propan-2-yl)carbamate (**9**)

To a solution of compound **8** (700 mg, 2.97 mmol), NMM (360.50 mg, 3.56 mmol) in THF (20 mL) was added IBCF (446.21 mg, 3.27 mmol) dropwisely at 0 °C. Then the mixture was stirred at 15 °C for 1 h. Then the mixture was added to aniline (331.92 mg, 3.56 mmol) at 0 °C. The mixture was stirred at

15 °C for 1 h and then was diluted with EA (50 mL), washed with 1M HCl (20 mL), H₂O (20 mL), brine (20 mL), dried over anhydrous Na₂SO₄, concentrated under reduced pressure to get compound **9** as a white solid.

White solid; Yield: 79%; Purity: 95%; ESI-MS: $m/z = 254.8[M+H-C_4H_9]^+$.

(*R*)-2-amino-3-(methylthio)-*N*-phenylpropanamide (**10**)

A solution of compound **9** (700.00 mg, 2.26 mmol) in DCM (10.00 mL) was added TFA (67.53 mmol, 5.00 mL), which was stirred at 15 °C for 1 h. The solvent was removed under reduced pressure to get the crude product as brown oil. The product was put into next step directly without further purification. Yield: 91%.

Preparation of (*R*)-*N*-(3-(methylthio)-1-oxo-1-(phenylamino)propan-2-yl)benzamide (**7c**)

To a mixture of compound **10** (700.00 mg, 2.16 mmol), NaHCO₃ (725.30 mg, 8.64 mmol) in THF (10 mL) and H₂O (5 mL) was added benzoyl chloride (425.08 mg, 3.02 mmol) at 0 °C. Then the mixture was stirred at 0 °C for 2 h. The solvent was removed under reduced pressure. The residue was diluted with DCM (50 mL), washed with 1 M HCl (20 mL), H₂O (20 mL), brine (20 mL), dried over anhydrous Na₂SO₄, concentrated under reduced pressure. The residue was purified by silicagel column (PE : EA = 5:1) to get compound **7c** as a white solid.

White solid; Yield: 61%; Purity: 96%; ¹H NMR (400 MHz, MeOD) : $\delta = 10.13$ (s, 1H, NH), 8.63 (d, $J = 7.5$ Hz, 1H, NH), 8.00 – 7.82 (m, 2H, Ar-H), 7.56 (ddd, 5H, $J = 31.8, 11.9, 4.2$ Hz, Ar-H), 7.34 (t, 2H, $J = 8.0$ Hz, Ar-H), 7.13 (t, 1H, $J = 7.4$ Hz, Ar-H), 3.06 (ddd, 2H, $J = 22.1, 13.8, 7.3$ Hz, CH₂), 2.22 (s, 1H, CH₃); ¹³C NMR (101MHz, DMSO): $\delta = 169.41, 166.46, 138.82, 133.84, 131.43, 128.69, 128.22, 127.54, 123.45, 119.35, 53.73, 35.29, 15.12$; HRMS (ES⁺) m/z 315.1064 (315.1089 Calcd for C₁₇H₁₈N₂O₂S M + H).

5.3 Pharmacology

5.3.1 Cell proliferation assay against hepatocellular injury model induced by H₂O₂

Human hepatocytes cell line, LO2 (provided by Shanghai Institutes for Biological Sciences, SIBS), was used to build hepatocytes injury model induced by H₂O₂ or APAP. The liver cell protective activities of target compounds were evaluated against hepatocellular injury model induced by H₂O₂, and Cell Counting Kit-8 (CCK-8, Beyotime, C0038) kit was utilized to detect the cell proliferation rates. Approximate 2×10⁶ LO2 cells were suspended in 10 ml fresh medium and cultured in the relative saturation humidity incubator in 5% CO₂ at 37 °C for 24 h. Then the culture liquid was removed and

300 μ L H₂O₂ fresh culture liquid with no fetal bovine serum (FBS) was added at the same condition for 6 h. The culture fluid was removed again, washed with phosphate buffered saline (PBS) for three times, and proceeded for trypsin digestion and suspending. Subsequently, the culture liquid was centrifuged with the supernatant abandoned, and then 1 ml PBS was added and the cells were suspended and counted. At last, the cells were transferred to 1.5 ml EP tube and centrifuged (4000 r \times 10 min). The supernatant was discarded and 150 μ L PBS was added for cell suspension, and then the cells were stored at -20 °C. All of the following procedures were carried out strictly accordance with the instruction of the CCK-8 kit. The absorbance was measured at 450 nm using a microplate reader. All the target compounds were screened against this cell model and the processing of the model group was similar to that of the compound test group, except that the tested compounds were not included in the hepatocellular injury cells induced by H₂O₂ when the CCK-8 kit was used. The results were calculated by using the GraphPad Prism 5.

5.3.2 Cell proliferation assay against hepatocellular injury model induced by APAP

The liver cell protective activities of selected compounds were evaluated against hepatocellular injury model induced by APAP, and CCK-8 kit was used to detect the cell proliferation rates. Similar to the injury model induced by H₂O₂, approximate 2×10^6 cells were suspended in fresh medium and cultured in 5% CO₂ at 37 °C for 24 h, then the culture liquid was removed and 1% DMSO plus 40 mmol APAP with no FBS was added for incubation with 5% CO₂ at 37 °C for 3 h. The following operation referred to the experimental procedures illustrated in paragraph 5.3.1.

5.3.3 *In vitro* MDA secretion assay

In this experiment, human normal LO2 cells were cracked directly and measured to determine the MDA level of normal group. The -20 °C stored cells (hepatocellular injury cells induced by H₂O₂ or APAP) were cracked with repeated freezing and thawing method, and the following assay was determined according to the instruction of the MDA kit (Beyotime, S0131). 0.37% thiobarbituric acid (TBA) storage liquid was prepared and the MDA detection work fluid was diluted according to the number of samples. 100 μ l (100 mmol) of various target compounds was added and treated with 200 μ M of MDA test solution. The processing of the model group was similar to that of the compound test group, except that the tested compounds were not included in the hepatocellular injury cells induced by H₂O₂ or APAP in the above experimental step. The solution was mixed at 100 °C for 15 min, cooled to room temperature and centrifuged (1000 g) for 10 min. Finally, the supernatant (200 μ l) was preloaded

in 96-well plate and the absorbance was determined by enzyme-meter 532.

5.4 ADME assay

5.4.1 Caco-2 permeability assay

Caco-2 cells (human colorectal adenocarcinoma line) were cultivated in MEM medium supplemented with 10% FBS, 1% non-essential amino acids solution and 0.1% penicillin/streptomycin in humidified atmosphere at 37 °C in 5% CO₂ and then were seeded at 4.8×10^4 cells/well on 24-well semipermeable insert plates (Millicell # PSHT 010 R5). The medium was changed every two days. After 21 days of cell growth the integrity of differentiated Caco-2 monolayers was verified by transepithelial electrical resistance (TEER) measurements using Millicell-ERS Voltammeter (Millipore # MERS 000 01). Caco-2 cell monolayers were considered acceptable for transport studies if the final values of TEER were greater than 250 Ω/cm^2 . For the permeability studies, 24-well insert plate was removed from its feeder plate and placed in a new sterile 24-well receiver plate. The cell layer was washed twice with HBSS (# 14025-092). In A-B direction, aliquots (400 μL) of the test compound solution (in duplicates, at 10 μM , in HBSS with 5.56 mM glucose buffered with 25 mM HEPES, pH 7.4) were added into the apical compartments of the trans-well insert and 1000 μL of the same buffer was added to the basolateral compartments; in B-A direction, aliquots (1000 μL) of the test compound solution (in duplicates, at 10 μM , in HBSS with 5.56 mM glucose buffered with 25 mM HEPES, pH 7.4) were added into the basolateral compartments of the trans-well insert and 400 μL of the same buffer was added to the apical compartments. The plates were then incubated for 1.5 h at 37 °C. High, low and Pgp substrate permeability controls (Atenolol, Metoprolol, Erythromycin) were run with every experimental batch to verify assay validity. The concentrations of the compounds tested in the permeability assay were determined using LC-MS-MS method. The formula for calculating Papp (expressed in 10^{-6} cm/s) was as follows:

$$P_{\text{app}} = (VA / (\text{Area} \times \text{time})) \times ([\text{drug}]_{\text{accepter}} / ([[\text{drug}]_{\text{initial, donor}}] \times \text{Dilution Factor}))$$

VA - the volume in the acceptor well, Area - the surface area of the membrane, time - the total transport time in seconds, $[\text{drug}]_{\text{accepter}}$ - concentration of test compound in the acceptor well, $[\text{drug}]_{\text{initial, donor}}$ - initial concentration of test compound in the donor well.

5.4.2 Pharmacokinetic studies

The protocol of rat pharmacokinetics study was reviewed and approved by the Institutional Animal Care and Use committee, Shanghai ChemPartner (protocol number: A998HL0002) prior to being

instituted, and the experiments were performed in accordance with the Guidelines for the Care and Use of Laboratory Animals at Shanghai ChemPartner Co., Ltd. The compounds were dissolved in 5% DMSO + 5% Solutol HS 15 + 90% (20% HP- β -CD in water) as a vehicle and were administered intravenously (i.v.) or orally (p.o.) to SD rats at 10 or 20 mg/kg. Ten male animals (bodyweight: 220-240 g) were used for i.v. or p.o. group, and blood was collected via tail vein at 5, 15, 30 min, 1, 2, 4, 8 and 24 h or 15, 30 min, 1, 2, 4, 8 and 24 h for i.v. or p.o administration, respectively. All animals had fasted overnight and fed 4 h post dosing and free access to water. EDTA-K2 was used as an anticoagulant, and blood sample was centrifuged at 4 °C (2000 g, 5 min) to obtain plasma within 15 min after sample collection. Plasma samples were analyzed after protein precipitation with ACN and centrifugation at 5800 rpm for 10 min using liquid chromatography coupled to mass spectrometry (LC-MS-MS) using appropriate calibration curves and an internal standard (Diclofenac) and bioanalytical quality controls. Pharmacokinetic parameters were calculated using Phoenix WinNonlin 6.4 software package (Pharsight) using non-compartmental analysis. Area under the plasma concentration versus time curve (AUC) was calculated by Linear Trapezoidal Linear Interpolation rule and bioavailability (BA, %) was calculated by $(AUC_{INF-PO} \times DOSE_{IV}) / (AUC_{INF-IV} \times DOSE_{PO}) \times 100\%$.

Conflict of interest

The authors confirm that this article content has no conflict of interest.

Acknowledgments

This study was supported by Grants from the Major science and technology innovation program of Hangzhou (Grant 20142013A60 and Grant 20152013A03), the Health care and key specialist scientific research project of Hangzhou Administration of Science and Technology (Grants 20150733Q49 and 20140733Q42),

References:

- [1] A. I. Shehu, X. C. Ma, R. Venkataramanan, *Clin. Liver Dis.* 2017, 21, 35-46.
- [2] K. Du, A. Ramachandran, H. Jaeschke, *Redox Biol.* 2016, 10, 148-156.
- [3] M. Maes, M. Vinken, H. Jaeschke, *Toxicol. Appl. Pharmacol.* 2016, 290, 86-97.
- [4] H. Wu, G. Zhang, L. Huang, H. Pang, N. Zhang, Y. Chen, G. Wang, *Oxid. Med. Cell Longev.* 2017,

363, 1565-1579.

- [5] Z. Gao, C. Zhang, W. Tian, K. Liu, R. Hou, C. Yue, Y. Wu, D. Wang, J. Liu, Y. Hu, Y. Yang, *Int. J. Biol. Macromol.* 2017, 97, 46-54.
- [6] S. Khan, R. N. Aljuhani, A. G. Morgan, A. Baghdasarian, R. P. Fahlman, A. G. Siraki, *Chem. Biol. Interact.* 2016, 244, 37-48.
- [7] Y. Hu, N. Zhang, Q. Fan, M. Lin, C. Zhang, G. Fan, X. Zhai, F. Zhang, Z. Chen, J. Yao, *Can. J. Physiol. Pharmacol.* 2015, 93, 625-631.
- [8] S. Penugonda, S. Mare, G. Goldstein, W. A. Banks, N. Ercal, *Brain Res.* 2005, 1056, 132-138.
- [9] R. Huang, Q. Pan, X. Ma, Y. Wang, Y. Liang, B. Dai, X. Liao, M. Li, H. Miao, *Stem Cells Int.* 2016, 2016, 8357567.
- [10] Z. H. Jiang, H. J. Lin, H. D. Yao, Z. W. Zhang, J. Fu, S. W. Xu, *RSC. Adv.* , 2017, 7, 15158-15167.
- [11] K. Kalimeris, P. Briassoulis, A. Ntzouvani, T. Nomikos, K. Papaparaskeva, A. Politi, C. Batistaki, G. J. Kostopanagiotou, *Surg. Res.* 2016, 206, 263-272.
- [12] K. Q. de Andrade, F. A. Moura, J. M. dos Santos, O. R. de Araújo, J. C. de Farias Santos, M. O. Goulart, *Int. J. Mol. Sci.* 2015, 16, 30269-30308.
- [13] N. Izigov, N. Farzam, N. Savion, *Free. Radic. Biol. Med.* 2011, 50, 1131-1139.
- [14] A. Khayyat, S. Tobwala, M. Hart, N. Ercal, *Toxicol Lett.* 2016, 241, 133-142.
- [15] N. V. Bhilare, S. S. Dhaneshwar, *Lett. Drug. Des. Discov.* 2017, 14, 209-215.
- [16] Y. Samuni, S. Goldstein, O. M. Dean, M. Berk, *Biochim. Biophys. Acta*, 2013, 1830, 4117-4129.
- [17] T. M. Farber, *Proc. Soc. Exp. Biol. Med.* 1975, 149, 13-18.

Figure captions:

Figure 1. Metabolic pathways affected by NAC and its molecular mechanisms

Figure 2. Design of novel NAC derivatives

Figure 3. Effect of NAC and target compounds on cell proliferation in H₂O₂ treated LO2 cells. (a) Viabilities of H₂O₂ treated LO2 cell line cultured with compounds **2a-e** and **3a-e**. (b) Viabilities of H₂O₂ treated LO2 cell line cultured with compounds **4a-e** and **5a-c**. (c) Viabilities of H₂O₂ treated LO2 cell line cultured with compounds **6a-c** and **7a-c**. **, significantly different from the model group

with $p < 0.01$; ***, significantly different from the model group with $p < 0.001$.

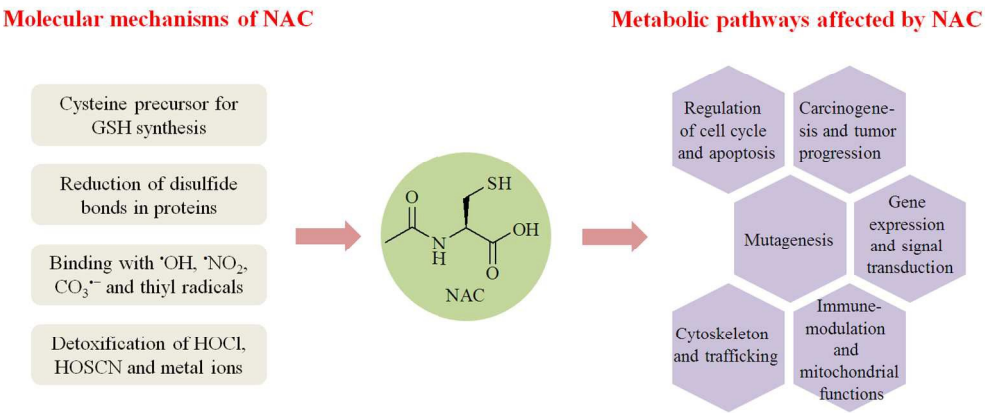
Figure 4. Effect of NAC and selected compounds on MDA secretion on H_2O_2 treated LO2 cells.

2.3 Cell viabilities and MDA secretion inhibitory activities on 4-Acetamidophenol (APAP) induced LO2 cell injury model

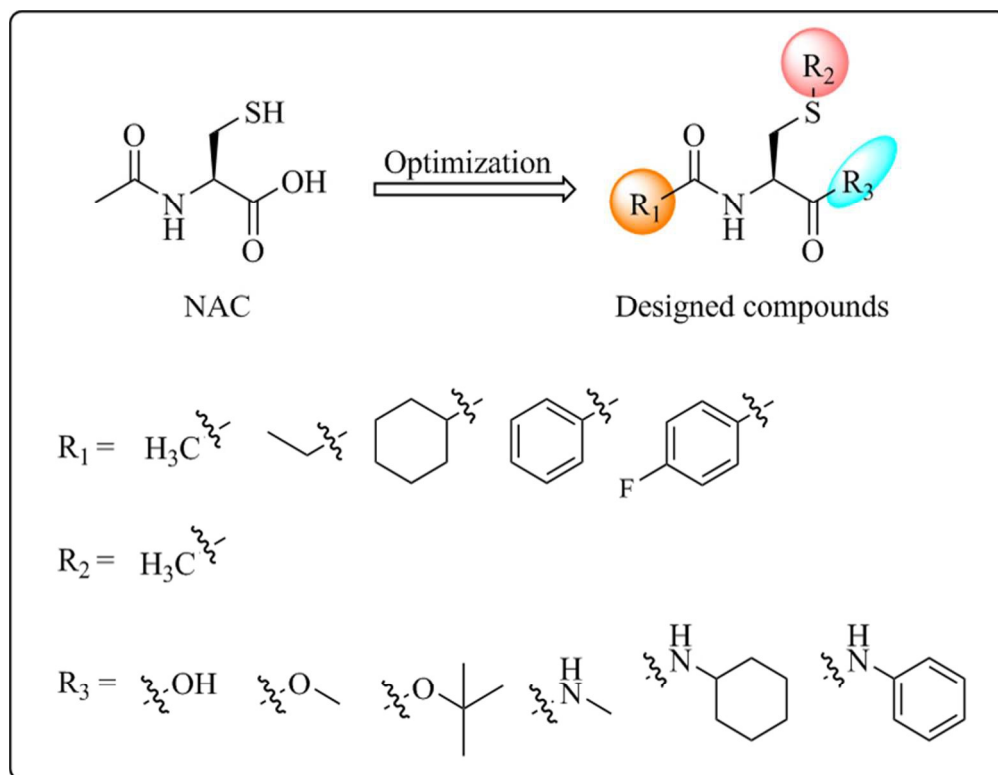
Figure 5. Effect of NAC and selected compounds on cell viability in APAP induced LO2 cells. *, significantly different from the model group with $p < 0.05$.

Figure 6. Effect of NAC and selected compounds on MDA secretion in APAP treated LO2 cells. ***, significantly different from the model group with $p < 0.001$.

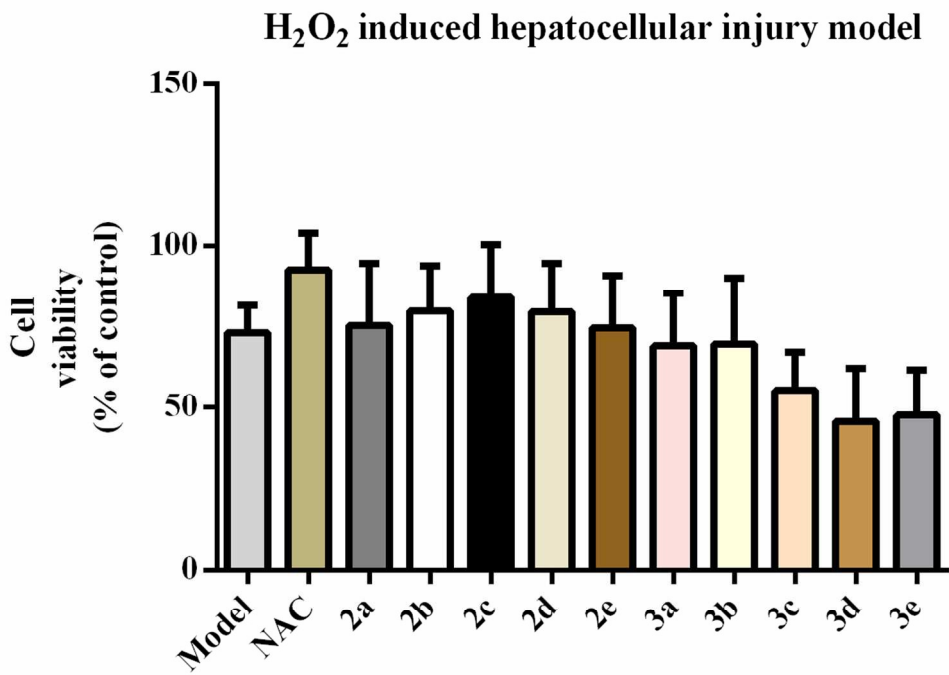
Scheme 1. Synthesis of target compounds **2a-e**, **3a-e**, **4a-e**, **5a-c**, **6a-c** and **7a-c**. Reagents and conditions: (I) DIEA, Fmoc-Cys(Me)-OH, NMM, DMF, DCM, rt; (II) HCl, MeOH, 15 °C; (III) 2-tert-butyl-1, 3-diisopropyl-isourea, DCM, 80 °C to rt; (IV) methylamine hydrochloride, EDCI, HOBt, DMF, DIEA, 15 °C; (V) NMM, IBCF, THF, 0 °C; (VI) aniline, HATU, DMF, 15 °C or aniline, EDCI, pyridine, 15 °C; (VIII) TFA, DCM, 15 °C; (IX) benzoyl chloride, $NaHCO_3$, THF, H_2O , 0 °C.



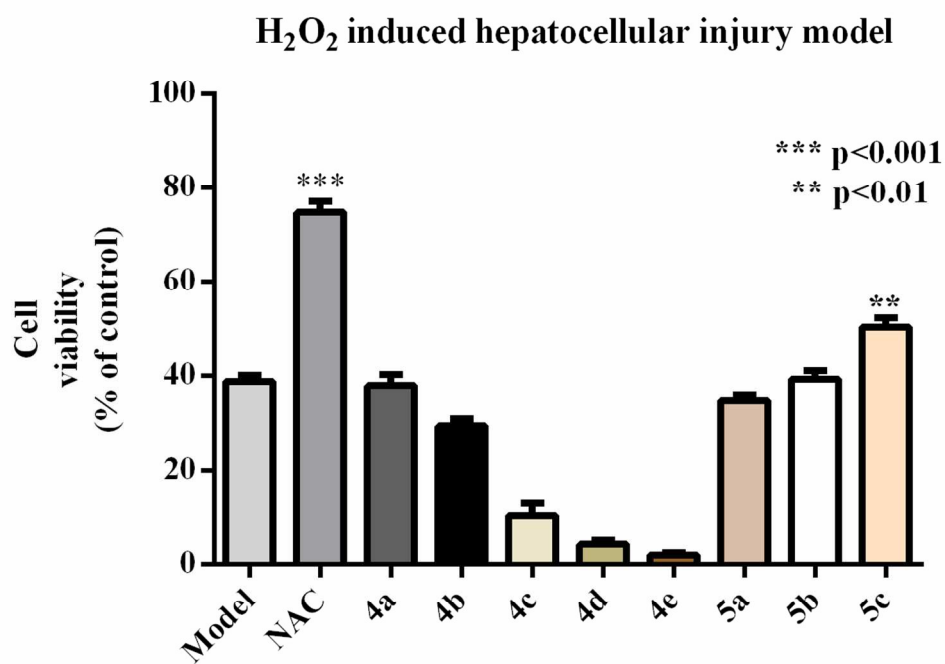
135x59mm (300 x 300 DPI)



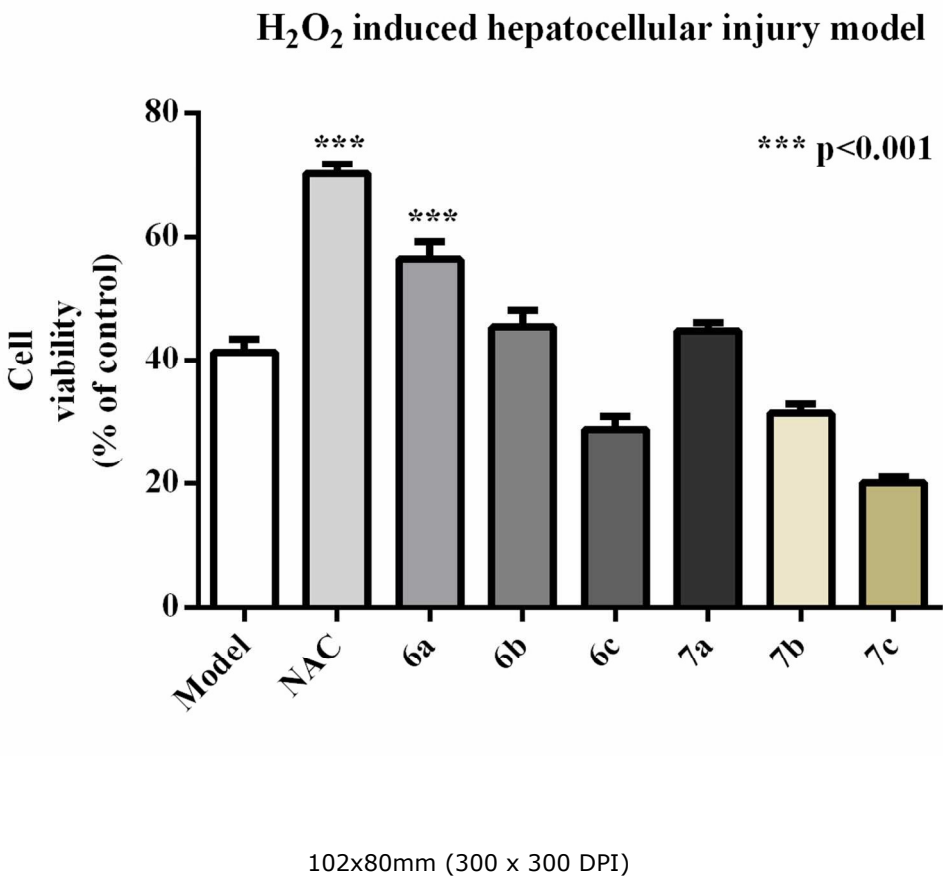
71x54mm (300 x 300 DPI)

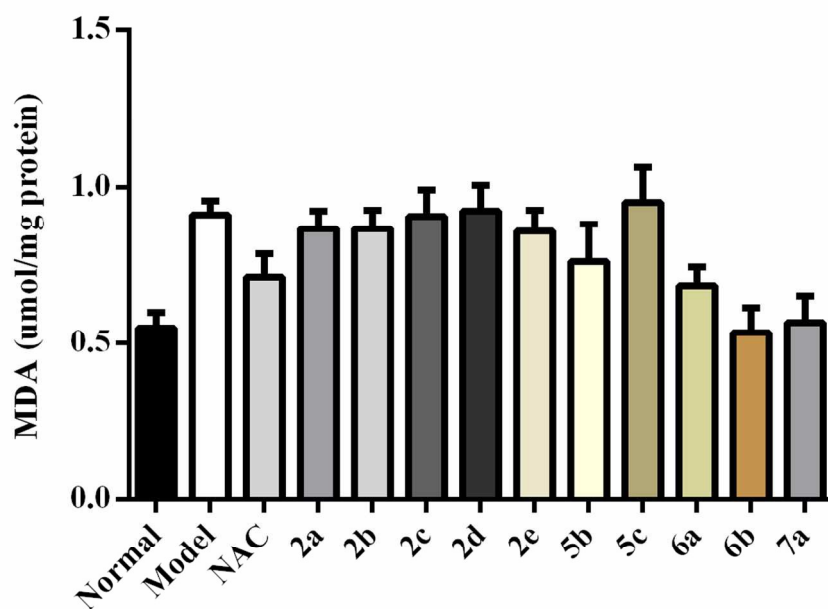


104x77mm (300 x 300 DPI)

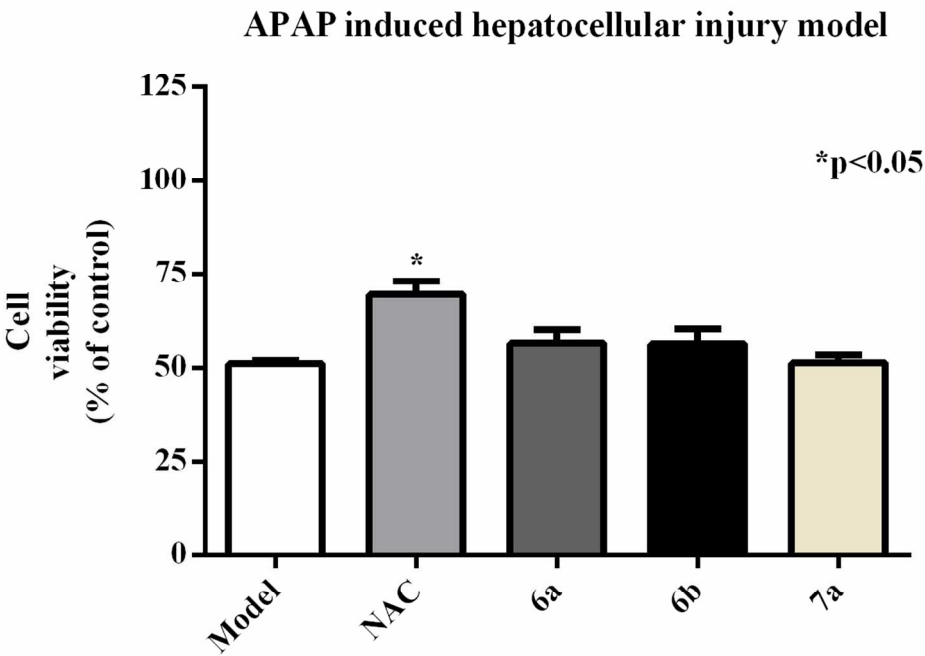


107x78mm (300 x 300 DPI)

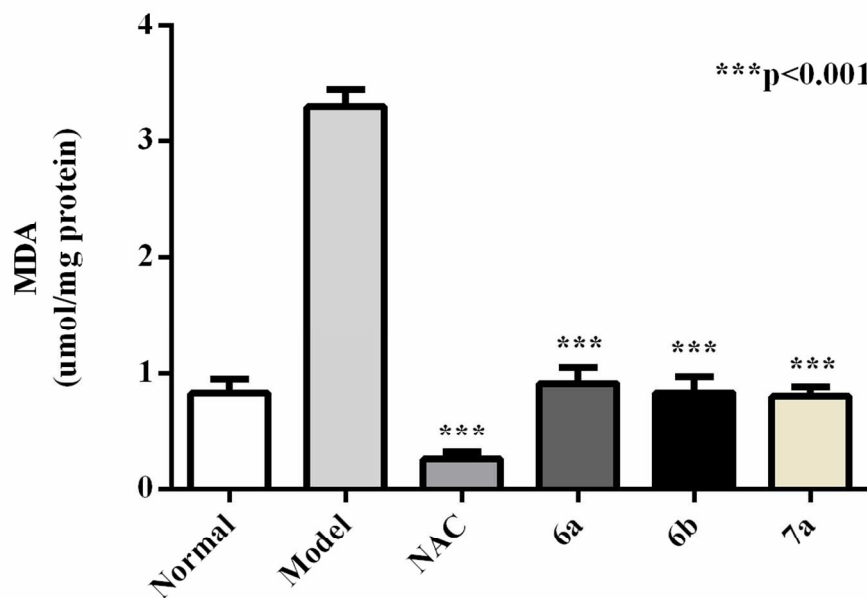


MDA secretion in H₂O₂ induced hepatocellular injury model

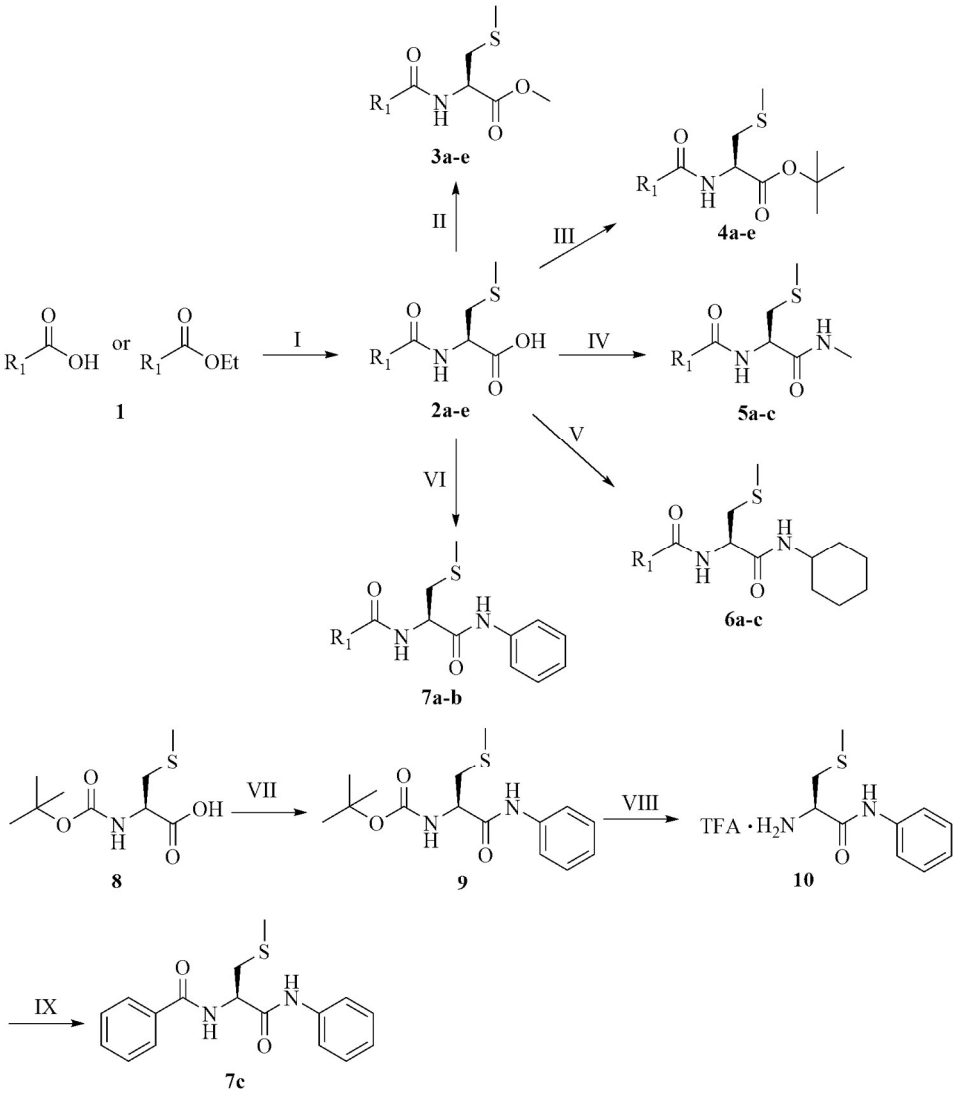
108x81mm (300 x 300 DPI)



108x78mm (300 x 300 DPI)

MDA secretion in APAP induced hepatocellular injury model

109x80mm (300 x 300 DPI)



2a, 3a, 4a, 6a, 7a R_1 = methyl 2b, 3b, 4b, 5a, 6b, 7b R_1 = ethyl 2c, 3c, 4c, 5b R_1 = cyclohexyl
2d, 3d, 4d, 5c, 6c, 7c R_1 = phenyl 2e, 3e, 4e R_1 = 4-fluorophenyl

154x194mm (300 x 300 DPI)

Table 1. Caco-2 permeability of compound **6a**

Compound	A-B permeability (Caco-2, $\text{cm} \cdot \text{s}^{-1}$) ^a (10^{-6})	B-A permeability (Caco-2, $\text{cm} \cdot \text{s}^{-1}$) ^a (10^{-6})	Papp(B-A)/ Papp(A-B)
6a	19.73	21.81	1.11
NAC	<1.09 ^b	<0.61 ^b	N/A

^a Each value is an average of $n = 3$, measured at $c = 10 \mu\text{M}$.^b Papp values were expressed as “<” than the values that were calculated using the minimum concentration of the standards for receiver sides due to the fact that real concentration in the receivers were below quantitation limit (BQL).

N/A: Not Acquired

Table 2. Pharmacokinetic data of compound **6a**

Compound	species	C _{max} (ng/ml) ^a	Terminal t _{1/2} (h) ^a	AUC (ng·h/ml) ^a	F(%) ^a
6a	SD rat ^b	2138±233	5.62±0.501	3082±446	52.8±4.64

^a Data represent means (n=5)

^b Male.